Contribution from the Department of Chemistry,
Brown University, Providence, Rhode Island 02912

Hydrogen Bonding in Metalloporphyrin Reactions. Reaction of (Tetraphenylporphinato)iron(III) Chloride and *N*-Methylimidazole

MARCA M. DOEFF and D. A. SWEIGART*

Received April 19, 1982

The reaction of *N*-methylimidazole, *N*-MeIm, and high-spin five-coordinate (tetraphenylporphinato)iron(III) chloride, Fe(TPP)Cl, proceeds rapidly to form low-spin Fe(TPP)(*N*-MeIm)$_2^+$Cl$^-$. During the reaction an intermediate mono(imidazole) complex, Fe(TPP)(*N*-MeIm)Cl, can be detected as a transient at room temperature and can be trapped for longer periods at low temperatures. The optical spectrum, ESR spectrum, and formation constant of the intermediate show it to be a high-spin six-coordinate species, proving that a spin change occurs upon addition of the second *N*-MeIm to form Fe(TPP)(*N*-MeIm)$_2^+$Cl$^-$. Kinetic studies in several solvents show that the rate-determining step in the reaction of *N*-MeIm and Fe(TPP)Cl is chloride ionization from the mono(imidazole) intermediate. The chloride ionization rate constant, k_1, is strongly dependent on the ability of the solvent to hydrogen bond to the departing chloride in the transition state as shown by a very good correlation of k_1 with Gutmann acceptor numbers for six solvents. Correlations do not exist with other common solvent parameters such as dielectric constant. Low concentrations of potential hydrogen bonders like trifluoroethanol and phenol have a large accelerating effect on k_1. The relationship between this work and possible hydrogen bonding involving distal and proximal histidines in hemoprotein-mediated reactions is discussed.

Introduction

Hydrogen bonding involving the axial ligands in the iron porphyrin prosthetic group of hemoproteins has recently been recognized as playing a significant role in structure and reactivity. The H bonding can be from an external protic source to an axially coordinated ligand or from a coordinated ligand (usually imidazole) to an external acceptor. For example, X-ray structures of hemoproteins show that the proximal histidine is always H bonded to other residues on the polypeptide backbone.[1] The variation of proximal H bonding has been proposed as a mechanism for altering the electron density at the metal and thereby the kinetics of trans ligand dissociation or association, the thermodynamics of trans ligand binding, the redox potential of the heme, and the ease of protein conformational change. H bonding by the proximal imidazole in hemoglobin (Hb) has been suggested as a mechanism for altering oxygen affinity and has been given a role in the cooperative binding of ligands. ESR studies,[2] MO calculations,[3] resonance Raman work,[4] and general observations[5,6] support the idea that proximal imidazole H bonding allows for electronic control of oxygen affinity. The stronger the H bond, the more negative charge donated to the iron from the coordinated imidazole, and this may favor oxygen binding through increased Fe → O_2 π back-bonding. The increased oxygen affinity in the R state of Hb compared to that of the T state may be due in part to increased proximal H bonding in the R state,[2-4] although recent work by Hoffman[7] supports greater H bonding for T-state hemoglobin.

In hemoproteins possessing a distal histidine, there is the possibility of H bonding to the axial ligand on the distal side. Such H bonding to dioxygen in HbO_2 and MbO_2 has been suggested as a way for the protein to stabilize the polar iron–dioxygen moiety, commonly formulated as coordinated superoxide Fe^{III}–O_2^-. Replacement of the E-7 histidine in the α chains of HbA by the potentially more strongly H-bonding tyrosine (as in HbM Boston) leads to facile autoxidation, which is probably due to H bonding strong enough to liberate superoxide: Fe^{III}–O_2^- → Fe^{III} + HO_2. It seems reasonable that the distal histidine in HbO_2 and MbO_2 H bonds to dioxygen strongly enough to stabilize the iron-bound O_2^- but not so strongly as to bring about proton transfer and formation of HO_2. If such H bonding is significant, it must affect the thermodynamics and probably also the kinetics of oxygenation. In a recent report Drago[8] showed that a good H bonder like trifluoroethanol markedly increases the oxygen affinity of cobalt(II) macrocycles. IR data suggested that this stabilization of the dioxygen adduct is due to H bonding of the trifluoroethanol to the coordinated dioxygen. Additional evidence for H bonding from a distal group is suggested by the similar O_2 binding strength in CoMb, CoHb, and Co(picket fence)(*N*-MeIm) compared to the much weaker binding in Co(PPIXDME)(*N*-MeIm) (where PPIXDME is the protoporphyrin IX dimethyl ester). The first three have a distal imidazole or amide N–H available for H bonding while the last example does not.

Although H bonding involving proximal or distal histidines plays a significant role in hemoprotein-mediated reactions, there is little quantitative information available to indicate the effect of this H bonding on the thermodynamics and kinetics of substrate–heme interactions. This report is the first in a series designed to quantify the importance of H bonding in the interactions of metalloporphyrins with ligands and solvent systems. The information obtained with these model systems should help our understanding of H bonding in hemoproteins, especially that involving proximal and distal histidines. In this report a mechanistic investigation of reaction 1 is presented.

$$\text{Fe(TPP)Cl} + 2N\text{-MeIm} \rightarrow \text{Fe(TPP)}(N\text{-MeIm})_2^+\text{Cl}^- \quad (1)$$

TPP is tetraphenylporphyrin and *N*-MeIm is *N*-methylimidazole. Thermodynamic studies of this and related reactions have been reported by several groups.[9,10] The five-coordinate Fe(TPP)Cl is high spin and the bis(imidazole) product is a low-spin ion pair in acetone and chloroform. The intermediate mono(imidazole) complex, Fe(TPP)(*N*-MeIm)Cl, is generally not seen in thermodynamic studies because the

(1) Landrum, J. T.; Hatano, K.; Scheidt, W. R.; Reed, C. A. *J. Am. Chem. Soc.* **1980**, *102*, 6729 and references therein.
(2) Chevion, M.; Salhany, J. M.; Castello, C. L.; Peisack, J.; Blumberg, W. E. *Isr. J. Chem.* **1977**, *15*, 311.
(3) Valentine, J. S.; Sheridan, R. P.; Allen, L. C.; Kahn, P. C. *Proc. Natl. Acad. Sci. U.S.A.* **1979**, *76*, 1009.
(4) Stein, P.; Mitchell, M.; Spiro, T. G. *J. Am. Chem. Soc.* **1980**, *102*, 7795.
(5) Caughey, W. S. In "Hemes and Hemoproteins"; Estabrook, R. E., Yonetoni, T., Eds.; Academic Press: New York, 1966.
(6) Mincey, T.; Traylor, T. G. *J. Am. Chem. Soc.* **1979**, *101*, 765.
(7) Stanford, M. A.; Swartz, J. C.; Phillips, T. E.; Hoffman, B. M. *J. Am. Chem. Soc.* **1980**, *102*, 4492.
(8) Drago, R. S.; Carmady, J. P.; Leslie, K. A. *J. Am. Chem. Soc.* **1980**, *102*, 6014.
(9) Walker, F. A.; Lo, M. W.; Ree, M. T. *J. Am. Chem. Soc.* **1976**, *98*, 5552.
(10) Coyle, C. L.; Rafson, P. A.; Abbott, E. H. *Inorg. Chem.* **1973**, *12*, 2007. Duclos, J. M. *Bioinorg. Chem.* **1973**, *2*, 263. Yoshimura, T.; Ozaki, T. *Bull. Chem. Soc. Jpn.* **1979**, *52*, 2268. Adams, P. A.; Baldwin, D. A.; Hepner, C. E.; Pratt, J. M. *Bioinorg. Chem.* **1978**, *9*, 479.

0020-1669/82/1321-3699$01.25/0

formation constant for the addition of the second imidazole (K_2) is much greater than that for the first addition (K_1), suggesting that the spin change occurs upon addition of the second imidazole. Walker[9] showed that imidazoles not substituted at the pyrrole nitrogen atom (N-1) have overall stability constants (β_2) about 10^3 times greater than with imidazoles lacking the N-1 hydrogen, e.g., *N*-MeIm. This important discovery was explained by postulating an extra stabilization of the N–H imidazole complexes through H bonding to the chloride or excess imidazole.

Pasternack[11] recently reported a kinetic study of reaction 1 in Me_2SO in which the Fe(TPP)Cl is known[12,13] to exist as the high-spin six-coordinate $Fe(TPP)(Me_2SO)_2^+$. The rate was found to be second order in *N*-MeIm, and no reaction intermediates could be detected. The analogous reaction with imidazole (HIm) was also second order and of similar rate. We have reported[14] some preliminary investigations of reactions of iron(III) porphyrin chlorides with imidazoles. With acetone as the solvent, in which the Fe(Por)Cl remains five-coordinate, we found the intriguing result that *N*-MeIm and HIm follow greatly different rates and rate laws. The rate is second order in HIm, but with *N*-MeIm as the nucleophile the kinetic behavior is more complex, being first order in *N*-MeIm at low concentrations and reaching zero order at high concentrations.

It was suggested that the difference between HIm and *N*-MeIm is due to assisted removal of the chloride by HIm via H bonding. This is not possible with *N*-MeIm and explains why the reactions are much faster with HIm. The mechanism proposed for HIm is shown in eq 2 and 3. Step 2 is the rapid

$$\text{Fe(Por)Cl} + \text{HIm} \overset{K}{\rightleftharpoons} \text{Fe(Por)(HIm)Cl} \qquad (2)$$

$$\text{Fe(Por)(HIm)Cl} + \text{HIm} \xrightarrow{\text{slow}} \text{Fe(Por)(HIm)}_2^+\text{Cl}^- \qquad (3)$$

formation of the mono(imidazole) complex. With *N*-PrIm as the nucleophile we found[14] direct spectroscopic evidence for its existence as a high-spin six-coordinate complex. In step 3 ionization of the chloride is assisted by H bonding from the HIm. With *N*-MeIm this step is unassisted. If this interpretation is correct, it shows that H bonding by imidazole can play a significant role in axial ligand activation, and if the bonding HbO_2 and MbO_2 is viewed as Fe^{III}–O_2^-, it suggests that H bonding from the distal histidine may significantly affect the thermodynamics and dynamics of oxygenation.

Although the H-bonding mechanism given above is attractive, an alternative one involving formation of the conjugate base monoimidazole intermediate, $Fe(Por)(Im)Cl^-$, is also reasonable. A detailed study of reaction 1 was undertaken to help distinguish between these mechanisms. The H-bonding mechanism predicts accelerated chloride ionization when a H bonder is present. Therefore, reaction 1 should be subject to general acid catalysis. Another reason for studying reaction 1 was to quantify solvent effects, particularly H-bonding properties, on the thermodynamics and kinetics of metalloporphyrin substitution reactions. A third reason for this work was to fully characterize the postulated mono(imidazole) complex, Fe(TPP)(*N*-MeIm)Cl.

Experimental Section

The rates and stability constants for reaction 1 are extremely sensitive to water and other protic materials. Since water is virtually a universal contaminant of organic materials, great care was taken to dry solvents thoroughly. Because *N*-MeIm is particularly hygroscopic, activated molecular sieves were added to all solutions. In general, the addition of activated 4-Å sieves to solvents and solutions was found to be a convenient and effective method for drying. Normal care was taken to protect solutions from atmospheric moisture and light.

N-MeIm was distilled from KOH pellets under reduced pressure. It was stored over molecular sieves and refrigerated. The bottle was allowed to come to room temperature before it was opened to prevent condensation of water. Aldrich Gold Label grade 2,2,2-trifluoroethanol was stored over $CaCl_2$ and was filtered directly prior to use. Tetrabutylammonium perchlorate was dried in vacuo prior to use. Tetrabutylammonium chloride was recrystallized from benzene–petroleum ether and dried in vacuo. All solvents were purified and dried according to well-known literature methods. When appropriate, this meant fractional distillation from P_2O_5, either under nitrogen or under air, with a drying tube attached to the still. In those solvents that were dried by less severe methods, activated sieves were added several hours before use. Some special comment is appropriate for two of the solvents, acetone and chloroform. Acetone is particularly difficult to dry and reacts slowly with many drying agents to give aldol condensation products and water. Acetone used for these experiments was allowed to sit over Drierite for several hours only. It was then distilled and dried over molecular sieves for 1 h. Chloroform is unstable with respect to its decomposition products, HCl, Cl_2, and phosgene. For this reason, a small amount of ethanol is added to the commercial products to prevent decomposition. The ethanol was removed from $CHCl_3$ by shaking several times with half its volume of distilled water, drying over $CaCl_2$ for 1 h, and then passing through a column of activated basic alumina to remove residual water and HCl. The purified solvent was never stored for more than $^1/_2$ h, since decomposition is fairly rapid. *Caution*: Storing chloroform purified in this manner for as short a period of time as 2 days may be dangerous due to the formation of poisonous phosgene gas. Even with these precautions, some HCl may still be present. All halogenated solvents were freshly distilled before use. Other solvents were used within several days of distillation.

Fe(TPP)Cl was purchased from Strem Chemical Co. and its purity verified via its visible spectrum. Fe(TPP)Br was made by shaking a solution of $(FeTPP)_2O$ in benzene with Baker-analyzed reagent grade hydrobromic acid (0.03% chloride). The visible spectrum of the reaction solution matched that reported[9] for Fe(TPP)Br and indicated that the reaction was quantitative. The solvent was evaporated and the solid taken up with diethyl ether, filtered, and washed. The resulting black powder was dried in vacuo for several hours. Elemental analysis (C, H, N, Cl, Br) indicated that this product was approximately 75% Fe(TPP)Br and 25% Fe(TPP)Cl.

Visible Spectra. Visible spectra were obtained for Fe(TPP)Cl and $Fe(TPP)(N\text{-MeIm})_2^+Cl^-$ in each solvent, with and without trifluoroethanol present. The visible spectra were virtually solvent independent. Spectra were recorded on a Gilford 250 spectrophotometer.

Kinetic Studies. The dynamics of reaction 1 were followed on a Dionex stopped-flow spectrophotometer, at 25 ± 0.5 °C. Low-temperature experiments were done on an all-glass stopped-flow apparatus designed[15] to allow immersion in a bath at any desired temperature. The kinetic experiments were made under pseudo-first-order conditions with the *N*-MeIm concentration ranging from 0.05 to 1.00 M and the iron porphyrin concentration at 5×10^{-5} M. The ionic strength of some solutions, as discussed in the text, was adjusted with tetrabutylammonium perchlorate to 0.136 M. Tetrabutylammonium chloride concentrations did not exceed 0.03 M. Reaction profiles were cleanly first order over several half-lives. Rate constants were evaluated from ln $(A - A_\infty)$ vs. time plots and standard least-squares fitting programs. Data obtained in chlorobutane was fitted to a nonlinear least-squares program. Activation parameters were calculated from a least-squares fit to the Eyring equation with rate data obtained over the temperature range +25 to −30 °C.

All rate profiles were repeated on different days to confirm reproducibility and the absence of water. Even traces of moisture can double or triple observed rates and lead to nonreproducible results. All reported rate constants were reproducible to within ±10%. Ca-

(11) Pasternack, R. F.; Gillies, B. S.; Stahlbush, J. R. *J. Am. Chem. Soc.* **1978**, *100*, 2613.
(12) Zobrist, M.; LaMar, G. N. *J. Am. Chem. Soc.* **1978**, *100*, 1944.
(13) Mashiko, T.; Kastner, M. E.; Spartalian, K.; Scheidt, W. R.; Reed, C. A. *J. Am. Chem. Soc.* **1978**, *100*, 6354.
(14) Burdige, D.; Sweigart, D. A. *Inorg. Chim. Acta* **1978**, *28*, L131. Fiske, W. W.; Sweigart, D. A. *Ibid.* **1979**, *36*, L429.
(15) The apparatus was designed and built by Dr. N. Rees, University College, Cardiff, United Kingdom.

Table I. Kinetic and Thermodynamic Parameters for Reaction 1 at 25 °C

solvent	dielectric const	AN[a]	k_1, s^{-1}	K_1, M^{-1}	$10^{-3}\beta_2$, M^{-2}
$CHCl_3$	4.7	23.1	360[b]	0.3[b]	1.1 ± 0.3
$ClCH_2CH_2CH_3CH_3$	7.4		0.7 ± 0.4	1.2 ± 0.6	0.008 ± 0.002
CH_2Cl_2	8.9	20.4	77 ± 3	2.7 ± 0.2	17 ± 4
CH_2ClCH_2Cl	10.4	16.7	29 ± 3	2.2 ± 0.2	12.9 ± 0.6
$CHCl_2CH_2Cl$			150 ± 40	0.8 ± 0.2	22 ± 5
CH_3COCH_3	20.7	12.5	3.5 ± 0.4	3.9 ± 0.3	6.6 ± 1.2
$C_6H_5NO_2$	34.7	14.8	17.8 ± 0.4	11.2 ± 0.5	3.4 ± 1.6
CH_3CN	38.8	19.3	110 ± 7	22 ± 2	very large

[a] Gutmann's acceptor number. [b] Estimated from data at lower temperatures; see text.

talysis profiles were obtained by using one or more constant concentrations of *N*-MeIm and varying trifluoroethanol concentrations (0 to 0.1 or 0.2 M). Second-order rate constants were obtained from the slopes of those lines. For some solvents trifluoroethanol concentration was held constant and *N*-MeIm concentration varied over the usual range. Second-order rate constants obtained from the limiting value of these plots agreed with those obtained by the first method.

Stability Constants. Static absorbance measurements at 25 °C were used to calculate β_2. Solutions were prepared that had a fixed metal concentration, various *N*-MeIm concentrations, and for some experiments various trifluoroethanol concentrations. The qualitative effect of trifluoroethanol on β_2 was determined by recording visible spectra of equilibrium mixtures having fixed metal and *N*-MeIm concentrations but varying trifluoroethanol concentrations.

Conductivity Measurements. Conductivity measurements were made with a Beckman Model RC-16B2 conductivity bridge and a Beckman dipping conductivity cell with a cell constant equal to 0.10 cm^{-1}. Dry acetone was used as the solvent. Measurements were made on solutions equilibrated at 25 ± 0.5 °C. The conductivity for pure solvent was subtracted from readings for all solutions; this amounted to about 1% of the total conductivity.

ESR Measurements. Spectra were recorded in frozen acetone at −170 °C on a Bruker ER-420 spectrometer.

Results and Discussion

Stability Constants. Conductivity measurements were made on Fe(TPP)Cl and Fe(TPP)(*N*-MeIm)$_2^+Cl^-$ solutions to determine the extent of chloride dissociation. Comparisons were made to conductivity data obtained with solutions of tetra-*n*-butylammonium chloride, for which ion-pairing constants are available.[16] The results indicate that at approximately 10^{-4} M Fe(TPP)Cl is totally associated in all solvents used and that Fe(TPP)(*N*-MeIm)$_2^+Cl^-$ is predominantly associated in solvents of low dielectric constants. In acetone (dielectric constant 20.7) Fe(TPP)(*N*-MeIm)$_2^+Cl^-$ at a concentration of 10^{-4} M is up to 50% dissociated.

Overall stability constants (β_2) for reaction 1 are given in Table I. No evidence for the mono(imidazole) intermediate was seen under equilibrium conditions. The β_2 values were obtained from standard Hill plots (eq 4). A_0 and A_∞ refer

$$\log \frac{A_0 - A}{A - A_\infty} = 2 \log [N\text{-MeIm}] + \log \beta_2 \qquad (4)$$

to the absorbances of Fe(TPP)Cl and Fe(TPP)(*N*-MeIm)$_2^+$-Cl^-, respectively. A is the absorbance of an equilibrium mixture, which was obtained as a function of *N*-MeIm concentration. Plots of eq 4 were linear with a slope of 2.0 ± 0.1 for all solvents. The intercept yielded β_2. With chlorobutane as the solvent β_2 is so low that A_∞ could not be obtained, and this necessitated the use of eq 5. A plot of A vs. $(A_0 - A)/[N\text{-MeIm}]^2$ was linear, the slope being $1/\beta_2$. In the use of eq 4 and 5, it is assumed that the product is primarily an ion pair, as the conductivity measurements show to be true except in the most polar solvents. To verify this, we used another equation (eq 6) to analyze the data, where ion dissociation is assumed. In principle eq 4 and 6 can be used to distinguish between an ion pair and free ions as the product in reaction 1. In practice, however, the data fit to eq 6 was only slightly less acceptable than the fit to eq 4. The stability constants reported in Table I assume the product is ion paired.

$$A = \frac{A_0 - A}{[N\text{-MeIm}]^2}\left(\frac{1}{\beta_2}\right) + A_\infty \qquad (5)$$

$$\log x = 2 \log [N\text{-MeIm}] + \log \beta_2'$$

$$x = \frac{(A_0 - A)^2 A_0}{(A - A_\infty)(A_0 - A_\infty)} \frac{1}{\epsilon_{Fe(TPP)Cl}} \qquad (6)$$

There is no simple relationship between β_2 for the reaction of Fe(TPP)Cl with *N*-MeIm and the dielectric constant of the medium. In addition, no semiquantitative relationship appears to exist between β_2 and empirical solvent parameters such as Reichhardt's E_T as previously believed.[9] The factors influencing β_2 are complex, including the relative stabilization of products by electrostatic and specific effects as well as the relative stabilization of the reactants. The lack of a good correlation with solvent parameters, which may only incorporate a few of these factors, is not surprising. However, some general observations can be made. In solvents such as benzene,[9] 1-chlorobutane, and toluene, where both dielectric constant and hydrogen-donating ability is low, formation constants are invariably small. Conversely, in solvents such as acetonitrile, which has a high dielectric constant and some ability to hydrogen bond, β_2 is very large. Apparently, both dielectric constant and hydrogen-donating ability are factors that influence the magnitude of β_2. The value of β_2 in chloroform shows that the effect of a low dielectric constant can be compensated for by the solvent's ability to H bond to the ionic chloride.

Addition of small amounts of an external H bonder such as trifluoroethanol was found to substantially increase β_2 in chlorobutane and acetone. This effect could not be quantitatively evaluated because β_2 was found to decrease with increasing *N*-MeIm concentration. This is probably due to H bonding between the *N*-MeIm and CF_3CH_2OH. Nevertheless, the qualitative effect of an added H bonder is to increase the extent of reaction 1, and this is likely due to product stabilization via H bonding to chloride.

Kinetics in Acetone. Reaction 1 occurs at a convenient speed in acetone to allow a thorough analysis of the dynamic behavior. Figure 1 shows typical results at 25 °C. During the rate study it was noted that in general the calculated absorbance change ($A_\infty - A_0$) and the observed change (ΔA_{obsd}) did not agree and at some wavelengths were of opposite sign. Furthermore the discrepancy between ΔA_{obsd} and $A_\infty - A_0$ was itself a function of the *N*-MeIm concentration. This is clear evidence for rapid reversible preequilibrium formation of an intermediate, which most reasonably is the mono(imidazole) complex, Fe(TPP)(*N*-MeIm)Cl. Assuming the preequilibrium refers to the addition of one *N*-MeIm per Fe(TPP)Cl, it was possible to calculate the formation constant (K_1) for the mono(imidazole) intermediate by fixing the Fe(TPP)Cl con-

(16) Savedoff, L. G. *J. Am. Chem. Soc.* **1966**, *88*, 664.

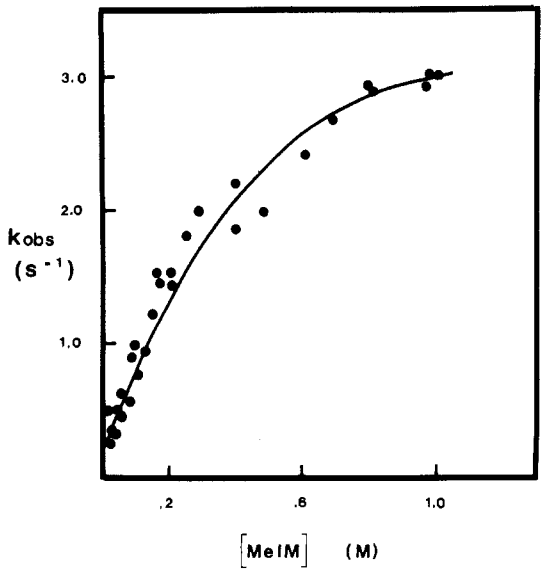

Figure 1. Rate constants for Fe(TPP)Cl + 2*N*-MeIm → Fe(TPP)(*N*-MeIm)$_2^+$Cl$^-$ in acetone at 25 °C.

centration and wavelength (535 nm) and varying [*N*-MeIm] and applying eq 7. A_1 is the absorbance of the intermediate.

$$A_\infty - \Delta A_{obsd} = -\frac{1}{K_1}\frac{A_\infty - A_0 - \Delta A_{obsd}}{[N\text{-MeIm}]} + A_1 \qquad (7)$$

A least-squares plot of eq 7 gave a good correlation. The slope yielded $K_1 = 4.0 \pm 0.9$ M^{-1}. The optical spectrum of the intermediate (A_1) was calculated as a function of wavelength according to eq 8, where $x = K_1[N\text{-MeIm}]/(1 + K_1[N\text{-MeIm}])$. The optical spectrum obtained by this point-by-point method was also measured directly by mixing precooled reactants and recording the spectrum in a low-temperature Dewar cell at −70 °C on a Gilford spectrophotometer. The results are given in Figure 2. At −70 °C the intermediate is stable for at least 10 min while at 25 °C it decays with a half-life of approximately 0.2 s. The intermediate spectrum obtained at −70 °C matches within error that obtained at 25 °C by use of eq 8.

$$A_1 = \frac{A_\infty - \Delta A_{obsd} - (1 - x)A_0}{x} \qquad (8)$$

With the above information about the existence and stoichiometry of the reaction intermediate, the mechanism given by eq 9–11 is postulated. After rapid preequilibrium formation of the mono(imidazole) complex, chloride ionization occurs and this ultimately yields the product. For the fully reversible mechanism shown in reactions 9–11, the calculated pseudo-first-order rate constant is shown in eq 12, where L is *N*-MeIm. Except at very low nucleophile concentrations or in chlorobutane as solvent (see below) the second term in eq 12 can be dropped. The data for all solvents except chlorobutane fit eq 12 well with the assumption $k_3[L] >> k_2$, so that the effective k_{obsd} is given by eq 13. The assumption $k_3[L] >> k_2$ merely means that the five-coordinate Fe(TPP)(*N*-MeIm)$^+$ is able to discriminate between the nucleophiles in favor of *N*-MeIm. Five-coordinate metalloporphyrins are known to have considerable discriminating ability.[17] The Fe(TPP)(*N*-MeIm)$^+$Cl$^-$ species may well be at least partially dissociated into free ions in acetone. If so, the addition of free chloride (as Bu_4NCl) could potentially cause a rate retardation. Experiments in acetone containing Bu_4NClO_4 to maintain constant ionic strength and Bu_4NCl to provide the free chloride showed that excess chloride has essentially no effect on the rate. This lends additional support to the abbreviated rate law in eq 13. It follows that the mechanism of reaction 1 can be simply described as rapid formation of a mono(imidazole) complex followed by rate-limiting chloride ionization.

$$\text{Fe(TPP)Cl} + N\text{-MeIm} \underset{}{\overset{K_1}{\rightleftharpoons}} \text{Fe(TPP)}(N\text{-MeIm})\text{Cl} \qquad (9)$$

$$\text{Fe(TPP)}(N\text{-MeIm})\text{Cl} \underset{k_2}{\overset{k_1}{\rightleftharpoons}} \text{Fe(TPP)}(N\text{-MeIm})^+\text{Cl}^- \qquad (10)$$

$$\text{Fe(TPP)}(N\text{-MeIm})^+\text{Cl}^- + N\text{-MeIm} \underset{k_4}{\overset{k_3}{\rightleftharpoons}} \text{Fe(TPP)}(N\text{-MeIm})_2^+\text{Cl}^- \qquad (11)$$

$$k_{obsd} = \frac{k_1K_1[L]}{1 + K_1[L]}\left(\frac{k_3[L]}{k_2 + k_3[L]}\right) + \frac{k_2k_4}{k_2 + k_3[L]} \qquad (12)$$

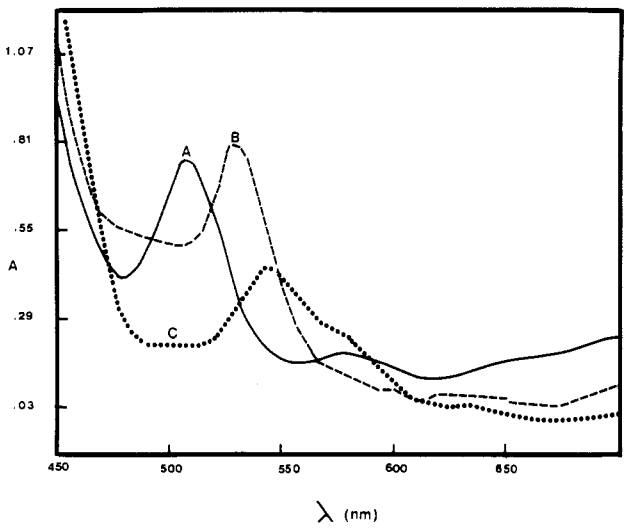

Figure 2. Spectra in acetone at −70 °C of (A) Fe(TPP)Cl, (B) Fe(TPP)Cl plus *N*-MeIm to give the intermediate Fe(TPP)(*N*-MeIm)Cl, and (C) solution B warmed to 25 °C and recooled to −70 °C to give Fe(TPP)(*N*-MeIm)$_2^+$Cl$^-$.

$$k_{obsd} = \frac{k_1K_1[L]}{1 + K_1[L]} \qquad (13)$$

A reciprocal plot of eq 13 yields (at 25 °C) $k_1 = 3.5 \pm 0.4$ s^{-1} and $K_1 = 3.85 \pm 0.3$ M^{-1}. This value of K_1 is seen to agree with that obtained by the *independent* method described above. The limiting rate constant k_1 was measured at five temperatures between −15 and +25 °C, and the standard Eyring plot gave the activation parameters $\Delta H^\ddagger = 9.7 \pm 0.5$ kcal/mol and $\Delta S^\ddagger = -24 \pm 4$ cal/(deg mol). The negative value of $\Delta S^\ddagger$ is expected[18] for an ionization process. A complete kinetic profile of reaction 1 in acetone at 15 °C gave $K_1 = 9.0$ M^{-1} at this temperature, showing that reaction 9 is exothermic.

The mono(imidazole) intermediate is a fairly rare example of a six-coordinate iron(III) porphyrin with one neutral and one anionic axial ligand. Several such complexes previously reported are known to be *low spin* and, when determined, to have quite large formation constants: Fe(TPP)(*N*-MeIm)N_3,[19] Fe(PPIX)(DMSO)CN,[20] Fe(TPP)(*N*-MeIm)SR,[21] and Fe-

(17) Martinsen, J.; Miller, M.; Trojan, D.; Sweigart, D. A. *Inorg. Chem.* **1980**, *19*, 2162. Levey, G.; O'Brien, P.; Prignano, A.; Sweigart, D. A., unpublished results.
(18) Moore, J. W.; Pearson, R. G. "Kinetics and Mechanism"; Wiley-Interscience: New York, 1981.
(19) Adams, K. M.; Rasmussen, P. G.; Schedit, W. R.; Hatano, K. *Inorg. Chem.* **1979**, *18*, 1892.
(20) Wang, J. T.; Yeh, H. J. C.; Johnson, D. F. *J. Am. Chem. Soc.* **1978**, *100*, 2400.

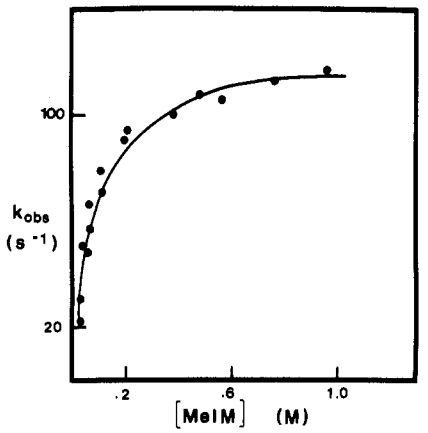

Figure 3. Rate constants for Fe(TPP)Cl + 2*N*-MeIm → Fe(TPP)(*N*-MeIm)$_2^+$Cl$^-$ in acetonitrile at 25 °C.

(PPIXDME)(*N*-MeIm)OR.[22] There is also a recent report[23] of high-spin complexes of Fe(PPIXDME)Cl with hindered 2-substituted imidazoles. To establish the spin state of the unhindered Fe(TPP)(*N*-MeIm)Cl complex, we prepared the intermediate in acetone solution at −70 °C by mixing the precooled reactants (excess *N*-MeIm). The solution was quickly frozen in liquid N_2 and its ESR spectrum recorded at −170 °C. The spectrum was that of a typical[24] high-spin ferric porphyrin ($g_\perp \approx 6.2$). This result confirms that the spin change in reaction 1 occurs upon addition of the second imidazole and explains why the formation constant K_1 is so small for Fe(TPP)(*N*-MeIm)Cl.

In order to confirm that the Fe(TPP)(*N*-MeIm)Cl intermediate contains six-coordinate iron and is not an ion pair, we attempted several experiments with Fe(TPP)Br. The Fe(TPP)Br was synthesized from HBr and (FeTPP)$_2$O in the usual manner.[25] Chemical analysis for Br and Cl indicated that a substantial amount of Fe(TPP)Cl was present as a contaminant. Chloride ion binds preferentially to the μ-oxo dimer, and there is enough chloride even in high-purity HBr to cause significant contamination of the Fe(TPP)Br product. The visible spectra of Fe(TPP)Br and Fe(TPP)Cl are indistinguishable, as are the spectra of the corresponding (*N*-MeIm)$_2$ adducts. It is possible that much of the work previously reported on Fe(TPP)Br was actually performed upon a mixture. Fe(TPP)Br used in this study was approximately 25% Fe(TPP)Cl. Reaction with *N*-MeIm in acetone gave a rate constant identical with that expected for Fe(TPP)Cl, but only one-fourth of the expected absorbance change was observed. This means that Fe(TPP)Br reacts much more rapidly than Fe(TPP)Cl with *N*-MeIm. This experiment essentially rules out the possibility that Fe(TPP)(*N*-MeIm)Cl exists as an ion pair. If it were an ion pair, one would expect the chloride and bromide to react at similar rates.

Kinetics in Other Solvents. Reaction 1 was studied in a number of solvents. The results are tabulated in Table I. All solvents except 1-chlorobutane gave rate behavior functionally the same as that obtained in acetone. Figure 3 gives a rate plot in acetonitrile. Due to the faster rates in most solvents compared to that in acetone, the K_1 formation constants could not be measured by static means as was done in acetone. The K_1 and k_1 values in Table I were calculated from fitting kinetic data to eq 13, except as noted below.

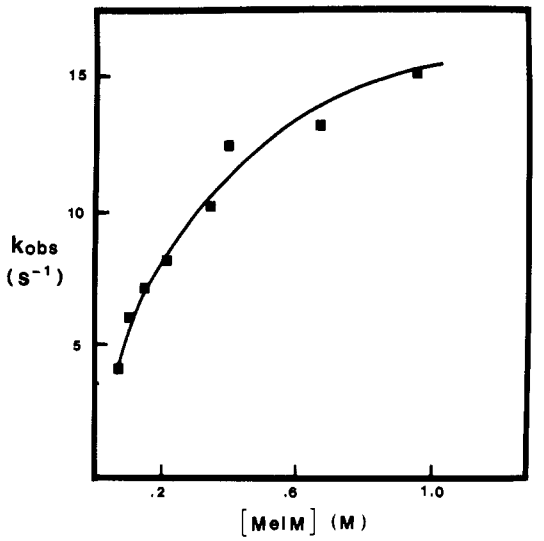

Figure 4. Rate constants for Fe(TPP)Cl + 2*N*-MeIm → Fe(TPP)(*N*-MeIm)$_2^+$Cl$^-$ in chloroform at −30 °C.

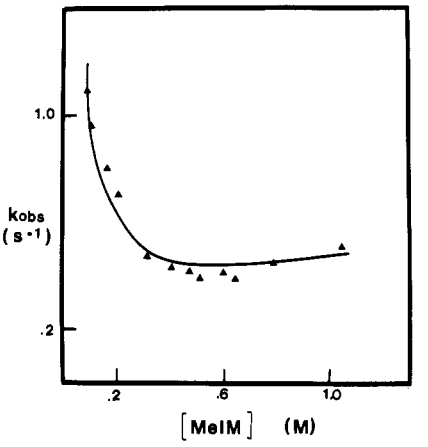

Figure 5. Rate constants for Fe(TPP)Cl + 2*N*-MeIm → Fe(TPP)(*N*-MeIm)$_2^+$Cl$^-$ in 1-chlorobutane at 25 °C.

At 25 °C, reaction 1 in $CHCl_3$ is too rapid to follow accurately by the stopped-flow method. Studies at −10 and −30 °C gave useful kinetic data. Figure 4 gives the results at −30 °C. With use of the observed values for K_1 and k_1 at −10 and −30 °C, the following kinetic and thermodynamic parameters were calculated: (k_1) $\Delta H^* = 7 \pm 2$ kcal/mol, $\Delta S^* = -22 \pm 6$ cal/(deg mol); (K_1) $\Delta H° = -6 \pm 3$ kcal/mol, $\Delta S° = -20 \pm 10$ cal/(deg mol). Extrapolation to 25 °C gives $k_1 = 360 \pm 180$ s^{-1} and $K_1 = 0.3 \pm 0.2$ M^{-1}.

The unusual rate behavior seen in 1-chlorobutane is shown in Figure 5. The observed rate constant at first *decreases* with [*N*-MeIm], reaches a minimum, and then increases. This behavior is in fact nicely consistent with the proposed mechanism. Because β_2 is very small in 1-chlorobutane, the observed approach to equilibrium is dominated by the reverse reaction when [*N*-MeIm] is small. In other words, the second term in eq 12 dominates. As [*N*-MeIm] increases, the two terms in eq 12 balance (the minimum in Figure 5) before the first term dominates at high [*N*-MeIm]. Nonlinear least-squares fitting to eq 12 gave the following results (25 °C): $K_1 = 1.2 \pm 0.6$ M^{-1}; $k_1 = 0.7 \pm 0.4$ s^{-1}; $k_3/k_2 = 44 \pm 35$; $k_4 = 4.8 \pm 6.3$ s^{-1}. The solid line in Figure 5 is the least-squares fit. The calculated curve is rather insensitive to k_4 and k_3/k_2, which explains the large errors associated with these constants.

Solvent Effects on k_1 and K_1. Unlike β_2, K_1 is not very solvent dependent. There is no correlation between K_1 and empirical solvent parameters or hydrogen-bonding ability and only a weak one between K_1 and the bulk dielectric constant.

(21) Tang, S. C.; Koch, S.; Papaefthymiou, G. C.; Foner, S.; Frankel, R. B.; Ibers, J. A.; Holm, R. H. *J. Am. Chem. Soc.* **1976**, *98*, 2414.
(22) Ainscough, E. W.; Addison, A. W.; Dolphin, D.; James, B. R. *J. Am. Chem. Soc.* **1978**, *100*, 7585.
(23) Yoshimura, T.; Ozaki, T. *Bull. Chem. Soc. Jpn.* **1979**, *52*, 2268.
(24) Subramanian, J. In "Porphyrins and Metalloporphyrins"; Smith, K. M., Ed.; American Elsevier: New York, 1975; Chapter 13.
(25) Bottomley, L. A.; Kadish, K. M. *Inorg. Chem.* **1981**, *20*, 1348.

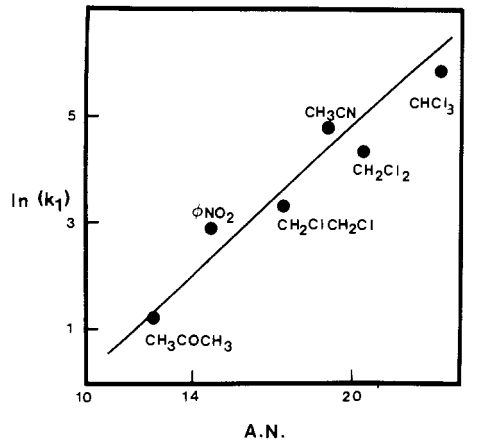

Figure 6. Correlation of chloride ionization rate constant, k_1, with Gutmann acceptor numbers.

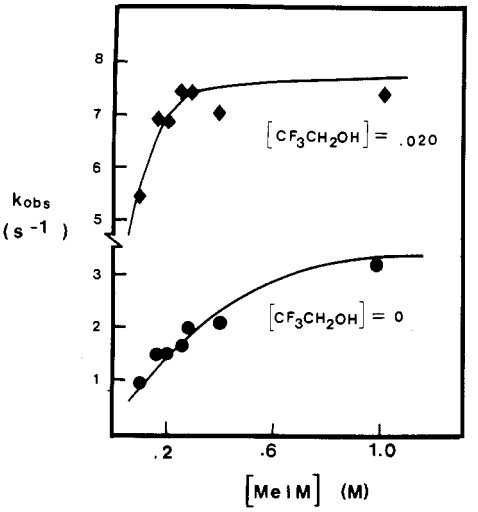

Figure 7. Effect of trifluoroethanol on Fe(TPP)Cl + 2*N*-MeIm → Fe(TPP)(*N*-MeIm)$_2^+$Cl$^-$ in acetone at 25 °C.

If K_1 involved chloride ionization, with or without dissociation, a much stronger dependence upon dielectric constant and hydrogen-bonding ability would be expected. This is dramatically illustrated by the contrasting increase in K_1 and β_2 upon going from 1-chlorobutane to acetone: K_1 increases by a factor of 3 and β_2 by a factor of 800. The variation of K_1 with solvent and the kinetic experiments described above provide a strong argument against the mono(imidazole) complex being an ion pair. Of course, it is quite possible that the Fe–Cl bond in Fe(TPP)(*N*-MeIm)Cl is somewhat more polar than in Fe(TPP)Cl, but it seems clear that the chloride is not essentially ionized.

In contrast to K_1, the rate constant k_1 is strongly solvent dependent. The variation cannot be explained by differences in dielectric constant alone. For example, k_1 in acetone is 3.5 s^{-1} and increases to 77 s^{-1} in methylene chloride. It was found that k_1 shows a surprisingly good correlation with Gutmann acceptor numbers (AN). Figure 6 illustrates this correlation. The Gutmann acceptor number (AN) is presumably a measure of the anion-solvating power of the solvent. It is determined from the ^{31}P NMR shifts produced upon transfer of triethylphosphine oxide through solvents.[26] This is a function of the ability of the solvent to accept electron pairs, which, in turn, is a function primarily of H-donating ability, although other solvent properties such as Lewis acidity and polarizability

(26) Gutmann, V. "The Donor-Acceptor Approach to Molecular Interactions"; Plenum Press: New York, 1978.

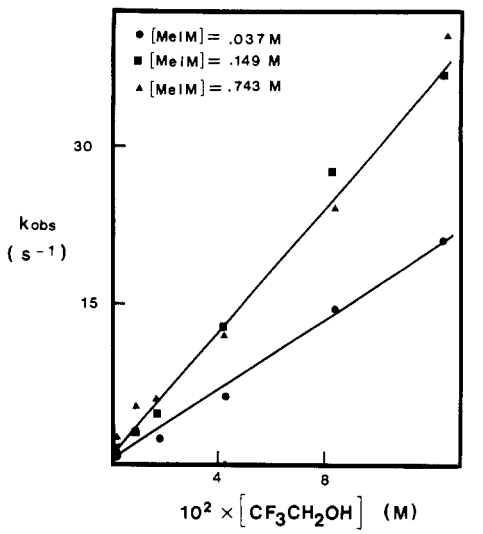

Figure 8. Rate constants for Fe(TPP)Cl + 2*N*-MeIm → Fe(TPP)(*N*-MeIm)$_2^+$Cl$^-$ as a function of trifluoroethanol concentration in acetone at 25 °C.

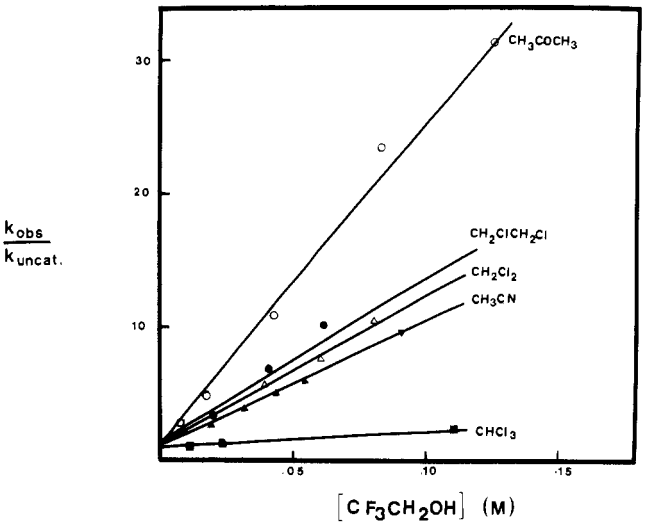

Figure 9. Plot of eq 15 in several solvents showing the effect of trifluoroethanol on the reaction Fe(TPP)Cl + 2*N*-MeIm → Fe(TPP)(*N*-MeIm)$_2^+$Cl$^-$. The methylimidazole concentration is 0.01 M for CH_3CN solvent and 0.15 M for other solvents.

can contribute with some solvents. This concept has found wide application in the interpretation of molecular interactions ranging from ionization equilibria and redox reactions of metal complexes to substitution reactions at carbon centers. A good correlation between AN and S_N1 solvolysis reactions has been reported by Parker.[27] Indeed, the slope of the plot in Figure 6 is almost the same as that for solvolysis of $(CH_3)_3CCl$.

The correlation of k_1 with AN and similarity to organic S_N1 solvolysis reactions strongly support the conclusion that k_1 refers to chloride ionization and that it is markedly accelerated by solvents that can H bond to the chloride as charge separation develops in the transition state. Pertinent to this suggestion is a recent paper by Romeo,[28] who showed that the rate of Pt–Cl bond cleavage in the cis–trans isomerization of *cis*-Pt(PEt$_3$)$_2$(*m*-MeC$_6$H$_4$)Cl is strongly dependent on the solvent H-bonding ability.

Effect of External H Bonders. The addition of small amounts of a good H bonder like trifluoroethanol or phenol

(27) Parker, A. J.; Mayer, U.; Schmid, R.; Gutmann, V. *J. Org. Chem.* **1978**, *43*, 1843.
(28) Romeo, R.; Minniti, D.; Lanza, S. *Inorg. Chem.* **1980**, *19*, 3663.

was found to have a large effect on the reaction rates. Figures 7–9 illustrate the effects with trifluoroethanol; similar results were obtained with phenol. These figures show that H bonders greatly increase the rate constants but do not change the overall functional form of the rate law. The mechanistic interpretation of these results is that the H bonder is catalyzing the chloride ionization step in eq 10.

In Figure 8 the three *N*-MeIm concentrations shown correspond to low, moderate, and large extents of preequilibrium saturation in eq 9. That the two largest *N*-MeIm concentrations give essentially identical rate curves suggests that in the presence of trifluoroethanol the formation constant K_1 is increased. The greater curvature in the upper curve in Figure 7 suggests the same thing. However, this interpretation is complicated by the probability of H bonding between *N*-MeIm and trifluoroethanol. Such H bonding would reduce the effective concentration of trifluoroethanol and be more important the greater the *N*-MeIm concentration. This can account for the coincidence of the rate constants at the two highest values of [*N*-MeIm] in Figure 8 and can also rationalize the different curvatures in Figure 7.

The plots of k_{obsd} vs. concentration of trifluoroethanol (or phenol) were approximately linear in all solvents, and can be represented by eq 14. Equation 14 can be normalized to give

$$k_{obsd} = k_{uncat} + k_{cat}[CF_3CH_2OH] \quad (14)$$

eq 15, which is shown in Figure 9 for several solvents. The

$$\frac{k_{obsd}}{k_{uncat}} = 1 + \frac{k_{cat}}{k_{uncat}}[CF_3CH_2OH] \quad (15)$$

slopes of these plots allow a quantitative comparison of the trifluoroethanol catalysis as a function of solvent. This ratio, k_{cat}/k_{uncat}, depends on solvent in the following manner: acetone (230) > CH_2ClCH_2Cl (160) > CH_2Cl_2 (120) > CH_3CN (90) > $CHCl_3$ (10). This order roughly follows the Gutmann AN values and is identical with the order for k_1, meaning that solvent can compete with the trifluoroethanol for H bonding to the chloride in the transition state for reaction 1, with $CHCl_3$ being the best H bonder.

Conclusions. This work shows that Fe(TPP)Cl reacts with *N*-MeIm in a stepwise fashion to give the bisadduct Fe(TPP)(*N*-MeIm)$_2^+Cl^-$, which is best described as an ion pair. The intermediate mono(imidazole) adduct can be detected as a transient during the reaction and for longer periods of time at low temperatures. The ESR spectrum of the mono(imidazole) complex shows it to be high spin ($S = {}^5/_2$), proving that the spin change in reaction 1 occurs upon addition of the second *N*-MeIm. Rate studies in various solvents strongly suggest that the mono(imidazole) intermediate is six-coordinate with a covalent Fe–Cl bond and that the rate-limiting step is ionization of the chloride from the intermediate.

The chloride ionization rate constant (k_1) is strongly dependent on the ability of the solvent to H bond to the departing chloride in the transition state. There is a good correlation to Gutmann acceptor numbers. Similar H bonding from added CF_3CH_2OH or C_6H_5OH in low concentrations has a large accelerating effect on k_1. H bonders, whether bulk solvent or added source, also affect the position of equilibrium of reaction 1.

The relationship of the present work to the possible H-bonding roles of proximal and distal histidines in hemoproteins is interesting. H bonding of the distal histidine to the axial ligand on the distal side in compounds of Hb, Mb, and peroxidases is a topic of debate.[29] This study of reaction 1 has shown in a quantitative manner how important H bonding from an external source to an axially bound ligand is in influencing reaction kinetics and thermodynamics. Experiments are planned that will extend this information to include a quantitative assessment of H bonding to axial ligands other than chloride, in particular dioxygen.

H bonding from metal-bound imidazole (proximal histidine) is a plausible way for the hemoprotein to modulate reactivity of trans-coordinated substrates. Work by Hoffman[7] has shown this to be important in Fe(II) heme–CO complexes. We noted some time ago[14] that reaction 1 followed different rate laws with HIm and *N*-MeIm as the nucleophile. The present work suggests that the difference is due to H bonding by HIm to chloride in the ionization step, reaction 10. However, a conjugate base mechanism, in which the coordinated HIm in the mono(imidazole) intermediate is H bonded or deprotonated by external HIm, is still a possible explanation. Experiments are planned that will probe this proximal H-bonding effect by intentionally trying to H bond the coordinated HIm to varying degrees and then measuring the effect on trans ligand activation.

Acknowledgment. We are grateful to Professor P. H. Rieger for writing a nonlinear least-squares program and to Professor J. O. Edwards for many stimulating discussions. We also thank Professor C. D. Baer for help in obtaining low-temperature spectra with a Gilford Model 2600 at Providence College. This work was supported by a BRSG grant from Brown University.

Registry No. Fe(TPP)Cl, 16456-81-8; Fe(TPP)(*N*-MeIm)Cl, 61056-71-1; Fe(TPP)(*N*-MeIm)$_2^+Cl^-$, 41121-76-0; *N*-MeIm, 616-47-7; trifluoroethanol, 75-89-8; phenol, 108-95-2.

(29) Perutz, M. F. *Annu. Rev. Biochem.* **1979**, *48*, 327.